REINFORCING EFFECT OF CARBON NANOTUBE (CNT) ON POLYMER NANOCOMPOSITES – A NUMERICAL-ANALYTICAL STUDY

A. Pantano[1 *]

[1] *Università degli Studi di Palermo, Dipartimento di Ingegneria Chimica, Gestionale, Informatica e Meccanica, Viale delle Scienze, 90128, Palermo, Italy*
** antonio.pantano@unipa.it*

Keywords: carbon nanotubes, numerical modeling, composites.

Abstract
A mixed model, numerical-analytical, is presented that allows one to predict the elastic properties of carbon nanotube (CNT)/polymer composites containing a random distribution of CNTs, while taking account of the curvature that they show when immersed in the polymer. This hybrid approach is a significant advance over micromechanical modeling and can be applied to all nanostructured composites.

1 Introduction
The sp^2 carbon-carbon bond in the basal plane of graphene is the stiffest and strongest in nature. Both experiments and atomistic simulations have confirmed that CNTs really have an extremely high modulus [e.g., 1-3] (Young's modulus > 1 TPa), and a strength around 100 GPa that is significantly higher than the few GPa of the carbon fibers. Carbon nanotubes also have a 5-20% elastic limit of the strain before failure and very low density ~1.75 g/cm3.
One way to take advantage of the marvelous properties of the carbon nanotubes consists in incorporating them into a matrix to build composite materials. The best candidates for this task are undoubtedly polymers, which thanks to their strength, toughness, low weight, and easy processing have been used in a broad variety of industrial application. The extraordinary mechanical properties, together with high ratios (100-10000) of geometric aspect, stiffness-to-weight, and strength-to-weight, all point to carbon nanotubes as potentially ideal reinforcing agents in advanced composites. The potential of the CNTs, as reinforcement structures, mainly depends on the ability to reach a homogenous dispersion within the matrix and to transfer the mechanical load from the matrix to the CNTs. If the CNTs are aggregated in a bigger structure, if the matrix deforms under loading, they will be separated in some smaller bundles without giving any significant contribute to the composite stiffness. When the cohesion at the interface between the phases is weak, the load is not transferred to the CNTs that will not be able to reinforce the matrix. In this case the CNTs behave like if they were holes or nanostructured defects. These difficulties hinder the production of high-performance composites based on CNTs. As a result, despite some encouraging results [for example, 4], there are many experiments showing only modest improvements in strength and in stiffness of the composites after the incorporation of the CNTs [for example 5-7]. Andrews et al. [5] got a limited increase of 15% in the elastic modulus, compared with the pure matrix, and a decrease in mechanical strength at a concentration of 5% volume fraction of multi-walled carbon

nanotubes (MWCNTs). Xia et al. [6] prepared obtained an increase in Young modulus of varying from 8.8% to 36%, using up to 3% in weight of CNTs. Similar results has been found by Song at al. [7]. The mechanical properties of composite were increased of 17% in stiffness using 1.5% in weight of CNTs. The small improvements mainly depend on the weak bond at the interface CNTs/matrix.

Many numerical models have been developed [8-11] in attempts to improve the understanding of the stiffening effects of CNTs in a polymer matrix. These studies are based on the micromechanical models, because the atomistic models are computationally too expensive to simulate the behavior of the composite. Each of these micromechanical models assumes perfect cohesion between CNTs and polymer matrix; this assumption determines that the predictions of the composite mechanical properties are highly optimistic compared with the experimental results. Commonly, at the interface between nanotubes and polymer, the interactions exist only by mean of the van der Waals bonds, that are able to produce only weak normal attraction forces, but they are not able to generate any significant sliding resistance, as has been investigated by Frankland et al.[12].

This article presents a new mixed model, numerical-analytical, which allows to predict the elastic characteristics of composites with random distribution of CNTs, taking into account the curvature that they show when immersed into the polymer. This hybrid approach represents an appreciable evolution over the micromechanical modeling [13-14] and can be applied to every nanostructured composites. To simulate the mechanical behavior of CNTs, a structural non linear model, previously developed [15], has been adopted; this model is a modified version of a known methodology, appreciated by the scientific community [16-19]. The approach, useful to investigate the CNTs deformations, is based on a finite element (FE) model, carefully developed basing on the knowledge of the spatial distribution of the carbon atoms in the nanotube structure and of the nature of the interatomic links. In this model the nanotubes properties are updated depending on the state of the local deformations.

The new methodology has been validated by comparison with the results of laboratory tests performed on epoxy resin-CNTs composites.

2. Numerical-Analytical Model

The model essentially consists of two sections: the first is strictly numerical while the second is analytical-theoretical. The numerical part consists of performing a set of seven FE analyses. In the analytical-theoretical part the output of the FE analysis is used as input for the Mori-Tanaka method, a highly reliable analytical tool for the prediction of elastic behavior of composite materials.

2.1. The Mori-Tanaka method

The Mori-Tanaka method allows the determination of the stiffness matrix of a composite material consisting of N phases randomly arranged in a three-dimensional space [20-22]. Each phase, representing a different type of inclusion, has his own geometry and elastic properties. The stiffness matrix of the multi-phase composite is calculated according to the Mori-Tanaka approach presented by Weng [22] by the following expression:

$$C = \left(f_0 C_0 + \sum_{r=1}^{N-1} f_r \left\{ C_r A_r^{dil} \right\} \right) \left(f_0 I + \sum_{r=1}^{N-1} f_r \left\{ A_r^{dil} \right\} \right)^{-1} \tag{1}$$

where C is the stiffness matrix of the N-phases composite, C_0 is the stiffness matrix of the resin, C_r is the stiffness matrix of the r-th inclusion, A_r^{dil} is the correlation matrix, or dilute

strain concentration tensor, of the r-th inclusion, I is the identity matrix , f_0 is the volume fraction of resin, f_r is the volume fraction of r-th inclusion.
The matrix A_r^{dil} correlates the volumetric average of the strains in the r-th inclusion, $\overline{\varepsilon}_r$, with those felt by the surrounding resin, or farflied strain tensor, $\overline{\varepsilon}_0$, as follows:

$$\overline{\varepsilon}_r = A_r^{dil}\overline{\varepsilon}_0 \tag{2}$$

$$A_r^{dil} = \left[I + S_r C_0^{-1}\left(C_r - C_0\right)\right]^{-1} \tag{3}$$

where the matrix S_r is the Eshelby tensor, whose form can be expressed in a closed form only for inclusions with simple geometry. In this work, the matrix A_r^{dil} is determined performing an appropriate set of FE analysis. In the case of CNTs-polymer matrix samples that we have manufactured for this study, the investigations performed using the SEM microscope showed that the arrangement of the nanotubes, embedded in the polymer, could be well approximated by a sinusoidal representation, see for example Figure 1 (a).

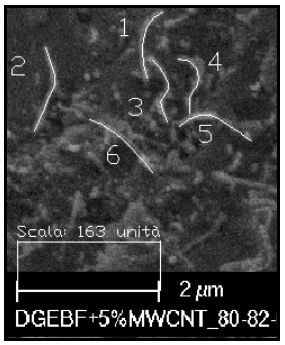

(a)


(b)

Figure 1. (a) Arrangement of nanotubes within the polymer matrix. Image obtained by SEM microscopy. (b) One of the samples in epoxy resin-MWNTs used for three-point bending tests.

Several images, obtained by SEM microscope investigation executed on the broken samples after the tests we carried out, show that the nanotubes population, in our samples, is well represented by an equivalent inclusion having sinusoidal pattern characterized by the following geometric parameters: wavelength λ = 800 nm, width 200 nm, outer diameter 30 nm, inner diameter 15 nm, number of sinusoid n = 2.
The expression (1), considering the case of a single equivalent inclusion, becomes:

$$C = \left(f_0 C_0 + f_1\left\{C_1 A_1^{dil}\right\}\right)\left(f_0 I + f_1\left\{A_1^{dil}\right\}\right)^{-1} \tag{4}$$

The quantities enclosed within the brackets {} have to be submitted to the randomization procedure, which allows taking into account the random distribution of the nanotubes embedded in the polymer. The equation (4) shows that to calculate the stiffness matrix of the composite, it's necessary to know the correlation matrix A_1^{dil} and the stiffness matrix of equivalent inclusion C_1. The determination of these quantities has been obtained by mean of a numerical set of six FE analysis to calculate the matrix A_1^{dil} and one further analysis to calculate the matrix C_1. A few important considerations need to be made regarding the Mori-Tanaka approach. The prediction of the Young's modulus from the original Mori-Tanaka approach [20-22] is not very accurate for large volume fraction, this is due to the fact that the method is based on a diluted homogenization scheme and that particle interactions is not

accounted for sufficiently. An estimate of the limits of the formulation can be found in the work of Schjodt-Thomsen and Pyrz [23], the Mori-Tanaka approach was found accurate up to a 15-20% volume fraction. Despite this limitation the new approach can be applied to a large number of composites since the CNTs are still extremely expensive and production of materials with a volume fraction of CNTs higher than 15-20% would be rarely justified by the increased performance of the composite. Moreover when the volume fraction of CNTs is high it is very difficult to obtain a good dispersion in the matrix.

2.1.1 Calculation of the correlation matrix A_1^{dil}

Rewriting in explicit form the equation (2), we obtain the following expression:

$$\begin{pmatrix} \overline{\varepsilon}_{r11} \\ \overline{\varepsilon}_{r22} \\ \overline{\varepsilon}_{r33} \\ \overline{\varepsilon}_{r23} \\ \overline{\varepsilon}_{r13} \\ \overline{\varepsilon}_{r12} \end{pmatrix} = \begin{bmatrix} A_{11} & A_{12} & A_{13} & A_{14} & A_{15} & A_{16} \\ A_{21} & A_{22} & A_{23} & A_{24} & A_{25} & A_{26} \\ A_{31} & A_{32} & A_{33} & A_{34} & A_{35} & A_{36} \\ A_{41} & A_{42} & A_{43} & A_{44} & A_{45} & A_{46} \\ A_{51} & A_{52} & A_{53} & A_{54} & A_{55} & A_{56} \\ A_{61} & A_{62} & A_{63} & A_{64} & A_{65} & A_{66} \end{bmatrix} \begin{pmatrix} \overline{\varepsilon}_{011} \\ \overline{\varepsilon}_{022} \\ \overline{\varepsilon}_{033} \\ \overline{\varepsilon}_{023} \\ \overline{\varepsilon}_{013} \\ \overline{\varepsilon}_{012} \end{pmatrix} \tag{5}$$

The equation (5) shows that, for the full knowledge of the matrix A_1^{dil}, 36 independent coefficients, of the type A_{ip}, must be determined. To this scope, an appropriate set of six FE simulations has been developed, to be performed on a representative volume element (RVE) of the material under consideration, consisting essentially of the nanotube immersed in the surrounding resin. In each of these six simulations, the RVE is subject to one of the six deformations $\overline{\varepsilon}_p$, of known value, imposed from outside of the RVE, assigning an appropriate displacement field to the external areas of the RVE such that the remaining deformations are zero and that one of interest assumes the desired value. After having resolved the analysis, in the post-processing step, it's possible to calculate the average deformations which the nanotube is subject to, using the following relation:

$$\overline{\varepsilon}_i = \frac{\int_V \varepsilon^i dV}{\int_V dV} \approx \frac{\sum_j \varepsilon_j^i v_j}{\sum_j v_j} \qquad r \in [1...6] \tag{6}$$

For each one of these six analyses, the expression (6) allows to determine all the six mean deformations which the nanotube is subject to and, thus, all the terms of the matrix A_1^{dil} using the following expression:

$$A_{ip} = \frac{\overline{\varepsilon}_i}{\overline{\varepsilon}_p} \qquad p \in [1...6] \tag{7}$$

2.1.2 Calculation of the stiffness matrix of the equivalent inclusion C_1

It has been assumed that the considered inclusion has got a macroscopically isotropic behavior and it's therefore characterized by a Poisson ratio ν = 0.19, experimentally verified for the CNTs, and an equivalent Young modulus E_{eq}, which takes into account the presence of a non-zero curvature, as that the nanotube has got a sinusoidal pattern. The determination of the equivalent Young modulus E_{eq} has been achieved performing a FE analysis, in which the

nanotube is located longitudinally in order to evaluate the stiffness of the sinusoidal waves train constituting the CNT.

2.2 FEM model design

2.2.1 RVE geometry

The considered model is a representative volume element (RVE), consisting of a CNT with a sinusoidal pattern immersed in a cube of epoxy resin which represents the matrix surrounding the inclusion.

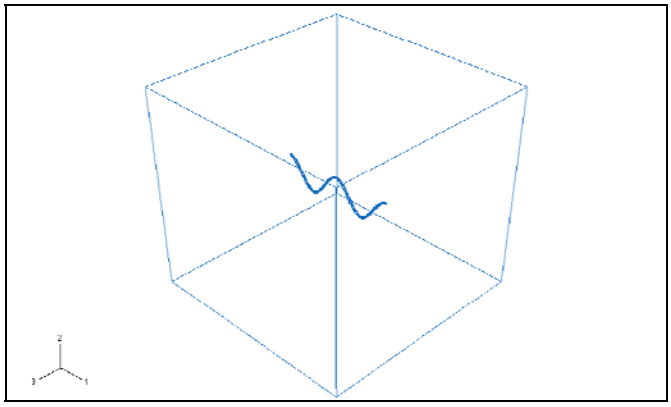

Figure 2. Representative Volume Element.

The CNT and the matrix are two separate elements that interact at the interface by mean of the presence of contact elements. Figure 2 shows the representative volume element. The matrix surrounding the nanotubes must be sufficient to avoid edge effects on the nanotube during the loading step, where a given displacement field is imposed to the external surfaces of the cube to cause the desired deformations. This condition requires that the ends of the nanotubes are sufficiently distant from the external faces of the resin cube. The parameter to be controlled is the volume fraction occupied by the nanotubes into the RVE. To achieve accurate simulations, this parameter must meet the following condition: $f_{CNT} \leq 0.05\%$.

2.2.2 Matrix constitutive model

The matrix is globally isotropic and is characterized by a linear-elastic behavior. In this case, we need to specify the following elastic constants; the resin used in our study, for the construction of the samples, has got the following characteristics: the Young module E_m=3620 MPa and the Poisson's ratio $v = 0.39$.

2.2.3 Carbon nanotube

The used model can be found in the literature [15] under the heading "EOR model" where EOR means "Equivalent Orthotropic Representation". The EOR model uses a micro-mechanical representation, in which the orthotropic planes are aligned with radial r, tangential θ and axial z directions of the nanotube.

2.2.4 Contact model

The considered model for the description of the nanotube-matrix contact, in the normal direction, allows us to transmit local forces of attraction between the nanotubes and the matrix, simulating, thus, the cohesion between the two materials. During each load increment if the tensile stress at the interface nanotube-matrix exceeds the value p_{min}, the two surfaces will be separated and the contact between them will be lost. The tensile stress p_{min} has been set equal to the maximum tensile stress that can occur between the walls of the MWCNT. It

has been obtained calculating the minimum of the law that describes the evolution of the pressure as a function of the distance between the walls:

$$p = \frac{\psi}{6}\left[\left(\frac{c_0}{c}\right)^{10} - \left(\frac{c_0}{c}\right)^{4}\right] \tag{8}$$

where $\psi = 3.65 \cdot 10^{-8}\left[\frac{N}{nm^2}\right]$ and $c_0 = 0.34\,[nm]$.

Minimizing the expression (8), we obtain: $p_{\min} = -1.98152 \cdot 10^{-9}\left[\frac{N}{nm^2}\right]$

2.2.5 Deformation mode

As mentioned, for the determination of the correlation matrix, it's necessary that the RVE is separately submitted to the three axial strains (ε_{11}, ε_{22}, ε_{33}) and to the three shear strains (ε_{12}, ε_{13}, ε_{23}).

2.2.6 Calculation of the equivalent Young modulus of the MWCNT

The determination of the equivalent Young modulus of the inclusion is performed fixing one of the two extreme CNT surfaces and applying to the other one a known displacement (in this case it has been chosen to impose $u_1 = 10$ nm). Measuring the average strain ε_{media}, along the axial direction of the nanotube, and the corresponding reaction force F, caused by the imposition of the required displacement, the equivalent Young modulus E_{eq} is determined.

2.2.7 Calculation of the Eshelby tensor

The post-processing step consists in elaborating the results contained in the report files of the FE analysis. The numerical result is:

$$A_1^{dil} = \begin{bmatrix} 0.1495 & 0.1053 & -0.1123 & 0.0004 & 0.0001 & 0.0131 \\ 0.1504 & 0.1449 & -0.0980 & 0.0003 & 0.0000 & -0.0139 \\ -0.1668 & -0.1167 & 0.2930 & -0.0009 & -0.0003 & 0.0012 \\ 0.0007 & 0.0007 & 0.0008 & 0.2574 & -0.0001 & 0.0005 \\ 0.0002 & -0.0002 & 0.0006 & 0.0000 & 0.2759 & -0.0007 \\ -0.0058 & 0.0003 & -0.0009 & 0.0002 & 0.0009 & 0.0957 \end{bmatrix} \tag{9}$$

$$C_0 = \begin{bmatrix} \frac{E_m}{1-\nu_m^2} & \frac{\nu_m E_m}{1-\nu_m^2} & \frac{\nu_m E_m}{1-\nu_m^2} & 0 & 0 & 0 \\ \frac{\nu_m E_m}{1-\nu_m^2} & \frac{E_m}{1-\nu_m^2} & \frac{\nu_m E_m}{1-\nu_m^2} & 0 & 0 & 0 \\ \frac{\nu_m E_m}{1-\nu_m^2} & \frac{\nu_m E_m}{1-\nu_m^2} & \frac{E_m}{1-\nu_m^2} & 0 & 0 & 0 \\ 0 & 0 & 0 & \frac{E_m}{2(1+\nu_m)} & 0 & 0 \\ 0 & 0 & 0 & 0 & \frac{E_m}{2(1+\nu_m)} & 0 \\ 0 & 0 & 0 & 0 & 0 & \frac{E_m}{2(1+\nu_m)} \end{bmatrix} \tag{10}$$

$$C_1 = \begin{bmatrix} \frac{E_r}{1-\nu_r^2} & \frac{\nu_r E_r}{1-\nu_r^2} & \frac{\nu_r E_r}{1-\nu_r^2} & 0 & 0 & 0 \\ \frac{\nu_r E_r}{1-\nu_r^2} & \frac{E_r}{1-\nu_r^2} & \frac{\nu_r E_r}{1-\nu_r^2} & 0 & 0 & 0 \\ \frac{\nu_r E_r}{1-\nu_r^2} & \frac{\nu_r E_r}{1-\nu_r^2} & \frac{E_r}{1-\nu_r^2} & 0 & 0 & 0 \\ 0 & 0 & 0 & \frac{E_r}{2(1+\nu_r)} & 0 & 0 \\ 0 & 0 & 0 & 0 & \frac{E_r}{2(1+\nu_r)} & 0 \\ 0 & 0 & 0 & 0 & 0 & \frac{E_r}{2\cdot(1+\nu_r)} \end{bmatrix} \tag{11}$$

where $E_m = 3620$ MPa, $\nu_m = 0.39$, $E_r = 6.0495 \cdot 10^4$ MPa and $\nu_r = 0.19$.
Rewriting the equation (3) explicating the Eshelby tensor S_1, we obtain:

$$S_1 = \left[\left(A_1^{dil}\right)^{-1} - I\right]\left[C_0^{-1}\left(C_1 - C_0\right)\right]^{-1} = \begin{bmatrix} 2.4785 & -0.0576 & 1.1999 & -0.0002 & 0.0010 & -0.3649 \\ -1.7092 & 1.0391 & -0.3590 & 0.0001 & -0.0010 & 0.3947 \\ 0.9281 & 0.5703 & 0.8378 & 0.0005 & 0.0004 & -0.0527 \\ -0.0056 & -0.0050 & -0.0055 & 0.1558 & 0.0000 & -0.0010 \\ -0.0045 & -0.0004 & -0.0027 & -0.0000 & 0.1417 & 0.0021 \\ 0.1724 & 0.0015 & 0.0862 & -0.0005 & -0.0018 & 0.4859 \end{bmatrix} \tag{12}$$

The knowledge of the Eshelby tensor allows us to predict the evolution of elastic properties of the composites as function of the volume fraction of nanotubes in solution.

3. Results

The batch of samples tested was composed of resin DGEBF, *diglycidyl ether of bisphenol-F*, and 5% volume fraction of MWNTs. The equation (4) shows how the composite stiffness matrix is only function of volume fraction of nanotubes in solution, because of all the other quantities appearing in it are known.

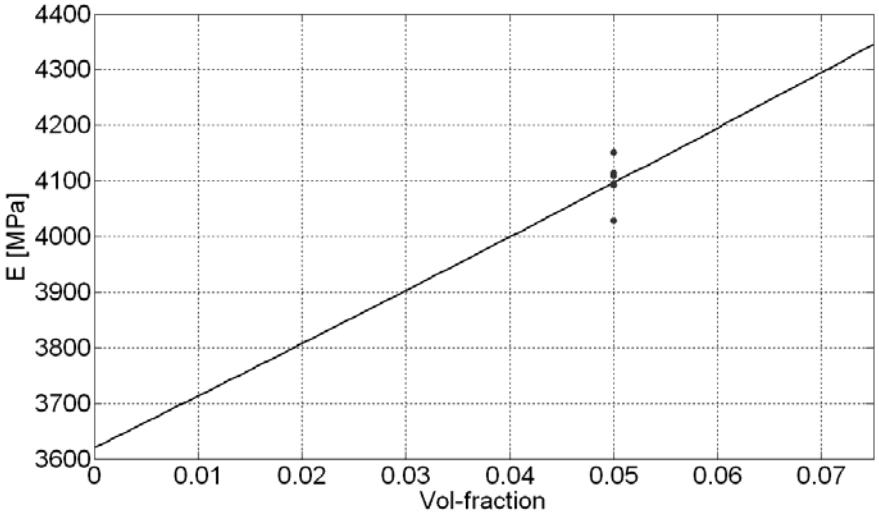

Figure 3. Trend of Young modulus of the composites as a function of the fraction of nanotubes. The black line shows the results predicted using the numerical-analytical model. The points corresponding to a volume fraction of 5% indicate the experimental results obtained testing composite samples.

It should be noted that the randomization procedure ensures that the composite stiffness matrix is the one of an isotropic material. In Figure 3 the black line shows the trend of the

composite Young modulus as a function of the CNTs volume fraction, predicted using the numerical-analytical model. The points corresponding to a volume fraction of 5% indicate the experimental results obtained testing composite samples. The Figure 3 shows a prefect agreement with the experimental results. In Figure 3, we see how the model provides a Young modulus of 4096.8 MPa at a volume fraction of 5%. This value is in excellent agreement with the mean value of Young modulus of the samples tested, which is 4097.9 MPa.

4. Conclusions

This article presents a new mixed model, numerical-analytical, which allows us to predict the elastic characteristics of composites with random distribution of CNTs, taking into account the curvature that they show when immersed in a polymer. The hybrid approach can be applied to every nanostructured composites. It has been validated by comparison with the results of laboratory tests performed on epoxy resin-CNTs composites. The model allowed us to investigate the influence of the CNTs volume fraction. The joint use of two methods, FEM and Mori-Tanaka, has enabled the development of a model that ensures high reliability in the prediction. The model is perfectly able to be adapted to the case where it's necessary to know the elastic characteristics of composites consisting of inclusions of different nature (forms and materials). In this case it will be necessary performing a set of seven FE analyses for each type of inclusion in the composite.

References

[1] J.N. Coleman, U. Khan, W.J. Blau, Y.K. Gun'ko: *Carbon*, **44**, 1624-1652, 2006.
[2] M. Moniruzzaman, K.I. Winey: *Macromolecules*, **39**, 5194-5205, 2006.
[3] O. Breuer and U. Sundararaj: *Polymer Composites*, **25**, 6, 630-645, 2004.
[4] D. Qian, E.C. Dickey, R. Andrews, T. Rantell: *Appl. Phys. Lett.*, **76**, 2868–2870, 2000.
[5] R. Andrews, D. Jacques, M. Minot, T. Rantell: *Macromol. Mat. and Eng.*, **287**, 395-403, 2002.
[6] H. Xia, Q. Wang, K.L., G.H. Hu: *J.l of Applied Polymer Science*, **93**, 378–386, 2004.
[7] Y.S. Song, J.R. Youn: *Carbon*, **43**, 1378–1385, 2005.
[8] G.M. Odegard, T.S. Gates, K.E. Wise, C. Park, E.J. Siochi: *Compos.Sci. Technol.*, **63**, 1671–1687, 2003.
[9] F.T. Fisher, R.D. Bradshaw, L.C. Brinson: *Compos. Sci. Technol.*, **63**, 1689–1703, 2003.
[10] R.D. Bradshaw, F.T. Fisher, L.C. Brinson: *Compos. Sci. Technol.*, **63**, 1705–1722, 2003.
[11] D. Shi, X. Feng, Y. Huang, K. Hwang, H. Gao: *J. of Eng. Mat. and Tech.*, **126**, 250-257, 2004.
[12] S.J.V. Frankland, A. Caglar, D.W. Brenner, M. Griebel: *J. Phys. Chem. B*, **106**, 3046-3048, 2002.
[13] A. Pantano, F. Cappello: *MECCANICA*, **43**, 263-270, 2008.
[14] A. Pantano, G. Modica, F. Cappello: *Mat. Science and Eng. A*, **486**, 222-227, 2008.
[15] M. Garg, A. Pantano, M.C. Boyce: *J. of Eng. Mat. and Tech.*, **129**, 431-439, 2007.
[16] A. Pantano, D.M. Parks, M.C. Boyce: *Phys. Rev. Lett.*, **91**, 145504, 2003.
[17] A. Pantano, M.C. Boyce, D.M. Parks: *J. Mech. Phys. Solids*, **52**, 789-821, 2004.
[18] A. Pantano, M.C. Boyce, D.M. Parks: *J. of Eng. Mat. and Tech.*, **126**, 279-284, 2004.
[19] A. Pantano, D.M. Parks, M.C. Boyce, M. Buongiorno Nardelli: *J. of Applied Physics*, **92**, 6756-6760, 2004.
[20] T. Mori, K. Tanaka: *Acta Metallurgica*, **21**, 571-574, 1973.
[21] Y. Benveniste: *Mechanics of Materials,* **6**, 147, 1987.
[22] G.J. Weng: *Journal of Engineering Science*, **28**, 1111-1120, 1990.
[23] J. Schjodt-Thomsen, R. Pyrz: Machanics of Materials, **33**, 531-544, 2001.